Séminaire Poincaré XII (2009) 75 – 88 Séminaire Poincaré

Evolution of Biological Complexity

Raymond E. Goldstein
Department of Applied Mathematics and Theoretical Physics
Centre for Mathematical Sciences
University of Cambridge
Wilberforce Road
Cambridge CB3 0WA, UK

Abstract. It is a general rule of nature that larger organisms are more complex, at least as measured by the number of distinct types of cells present. This reflects the fitness advantage conferred by a division of labor among specialized cells over homogeneous totipotency. Yet, increasing size has both costs and benefits, and the search for understanding the driving forces behind the evolution of multicellularity is becoming a very active area of research. This article presents an overview of recent experimental and theoretical work aimed at understanding this biological problem from the perspective of physics. For a class of model organisms, the Volvocine green algae, an emerging hypothesis connects the transition from organisms with totipotent cells to those with terminal germ-soma differentiation to the competition between diffusion and fluid advection created by beating flagella. A number of challenging problems in fluid dynamics, nonlinear dynamics, and control theory emerge when one probes the workings of the simplest multicellular organisms.

1 Introduction

One of the most fundamental issues in evolutionary biology is the transition from unicellularity to multicellularity, in which basic questions concern the fitness advantages conferred by increasing size and specialization [1, 2, 3, 4, 5]. To put this question in perspective, consider the data shown in Fig. 1, originally presented by Bell and Mooers [6] and discussed more recently by Bonner [3]. Unicellular organisms, which of course do all the functions of life with one cell type, reside at the lower left corner of this graph, while humans, with approximately 210 distinct cell types and 10^{14} cells, are at the upper right. Clearly, there is a general trend that organisms with larger total numbers of cells have more cell types, but there are wide variations among the different groups of organisms, and one would be hard-pressed to look for some precise mathematical scaling in this data. Instead, let us look at the most elementary steps along the path toward biological complexity: the transition from single cell organisms to those with just two distinct cell types.

Not surprisingly for microorganisms living in an aqueous environment, many of the key biological processes involved with this transition involve transport and mixing, for the efficient exchange of nutrients and metabolites with the environment is one of the most basic features of life [7]. In the conventional biological view, diffusion dominates over transport by fluid advection, as quantified by the Péclet number [8]

$$Pe = \frac{UL}{D} \ , \tag{1}$$

where U is a characteristic fluid velocity, L is a typical length scale, and D is the molecular diffusion constant of interest (typically 10^{-5} cm^2/s for small molecules such as oxygen, and varying inversely with size). The low Pe number world is most appropriate to small individual organisms such as bacteria [9], where $L \sim 10^{-4}$ cm and $U \sim 10^{-3}$ cm/s, so $Pe \sim 10^{-2}$. Such is generally not the case for multicellular organisms whose size L and swimming speed U are considerably larger. In a nutshell, this presentation concerns the relationship between advection and evolutionary transitions to multicellularity – what might be termed "Life at High Péclet Numbers."

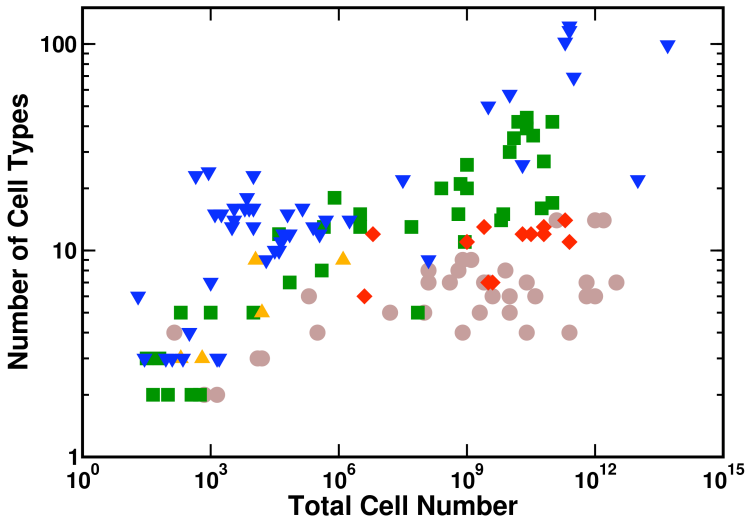

Figure 1: Scaling of the number of distinct cell types with total number of cells in various organisms. Data include amoebas, ciliates and brown seaweeds (brown), green algae and plants (green), red seaweeds (red), fungi (orange), and animals (blue). Adapted from Bells and Mooers [6] and Bonner [3].

2 *Volvox* and its Relatives as Model Organisms

Long after he made his great contributions to microscopy and started a revolution in biology, Antony van Leeuwenhoek peered into a drop of pond water and discovered one of nature's geometrical marvels [10]. This was the freshwater alga which, years later, in the very last entry of his great work on biological taxonomy, Linneaus named *Volvox* [11] for its characteristic spinning motion about a fixed body axis. In van Leeuwenhoek's drawing (Fig. 2) we see that *Volvox* is a spherical colonial green alga with thousands of surface cells and daughter colonies inside the spheroid. His microscopy was insufficient to determine that *Volvox* swims by means of two beating flagella on each of the surface cells. We now know that those flagella are nearly identical to the cilia in our lungs. Indeed they are one of the most highly conserved structures in biology, a testament to the importance of fluid dynamics in life at all scales.

Over a century ago, Weismann [12] suggested that a set of organisms related to *Volvox*, known as the Volvocine algae, can serve as a model lineage for study of the transition from unicellular to multicellular organisms, an argument amplified more recently by Kirk [13]. This suitability derives from the fact that this *extant* lineage (Fig. 3) displays varying colony size, structure, and specialization into the two fundamental cell types: vegetative (soma) and reproductive (germ). The species include unicellular *Chlamydomonas*

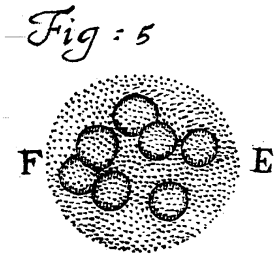

Figure 2: Figure 5 from van Leeuwenhoek's article on *Volvox* from 1700 [10]

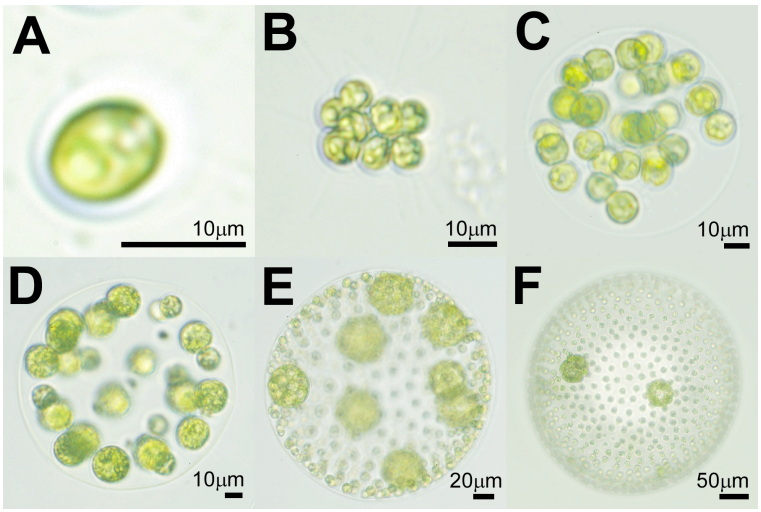

Figure 3: Volvocine species [22].

reinhardtii (A), undifferentiated *Gonium pectorale* (B) and *Eudorina elegans* (C), soma-differentiated *Pleodorina californica* (D), germ-soma differentiated *Volvox carteri* (E), *V. aureus* (F), and even larger (e.g. *V. gigas* with a radius of 1 mm). In the multicellular forms from *Volvox* upward in size the *Chlamydomonas*-like somatic cells are at the surface of a transparent, spherical extracellular matrix (ECM), with their two outward-oriented flagella conferring motility, while the reproductive cells/daughter colonies are sequestered on the inside of the ECM. A central question in the study of this lineage is: *What are the driving forces which led to the scale of* $\sim 150\ \mu m$ *for the onset of germ-soma differentiation?*

Although the precise relationships among species are not fully resolved in the Volvocales, it is known that *Volvox* species with increased cell specialization do not have a single origin - they have evolved several times, independently, from quite different ancestors [14, 15, 16, 17]. Lineages exhibiting the different developmental programs (details of cell division) [18] are interspersed with each other and with non-*Volvox* species, indicating that they have also evolved several times independently. Supporting this evidence for ease of evolutionary transitions is the underlying genetic architecture responsible for the separation of germ and soma, which does not involve many genetic steps [19]. Only two mutations are required to transform *V. carteri* into a mutant (*V. carteri* $glsA^{-}/regA^{-}$) with morphological and life-history features similar to those of *Eudorina* colonies with no

cellular differentiation [20]. In short, the Volvocales comprise a group of closely related lineages with different degrees of cell specialization which seem to represent "alternative stable states" [21].

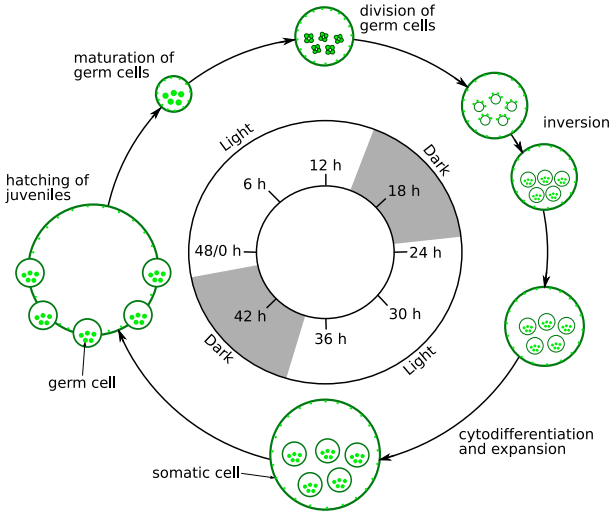

Figure 4: The 48 hour life cycle of *Volvox*, adapted from Kirk [13].

The tremendous range of size presented by these species, their common structural element of biflagellated somatic cells, and their most elementary differentiation beyond a critical size suggest that they would allow us to deconstruct scaling laws in self-propulsion, fluid mixing, and metabolism which may help explain the evolutionary driving forces which led to multicellularity. In the laboratory, *Volvox* is typically grown on a 48-hour lifecycle (Fig. 4). Populations can be rather precisely synchronized, so that large numbers are available at any given time in a well-defined life cycle stage, allowing for good statistical sampling of the properties during growth.

Volvox is also amenable to precise quantitative study of its fluid mechanics, using techniques from physiology. For instance, glass micropipettes familiar from *in vitro* fertilization, can be used to hold individual colonies under the microscope so that the flow fields produced by their collective flagellar beating can be mapped. Figure 5 shows an example of such a flow field, which shows clearly the existence of a (fixed) colonial axis, the flow along the surface being primarily from anterior to posterior. The flagella beat with a slight tilt, producing the force that makes the colony spin about its axis. In Fig. 5 we also observe that the characteristic length scale of these flows is comparable to the colony radius, and hence up to a fraction of a millimeter. The typical fluid velocities can reach nearly 1 mm/s, leading to Péclet numbers in the several hundreds, as anticipated above.

3 The Advection-Diffusion Problem

For these organisms, basic considerations point to an intrinsic bottleneck to nutrient uptake by diffusion alone [22, 23, 24]. For a spherical absorbing colony of radius R in a *quiescent* fluid medium, taking up a nutrient from a diffusional steady state concentration profile $C(r) = C_\infty\,(1 - R/r)$, where C_∞ is the concentration far away, the diffusional current I_d of nutrients is linear in the radius: $I_d = 4\pi D C_\infty R$. In contrast, the metabolic requirements of surface somatic cells will scale as $I_m = 4\pi R^2 \beta$, where β is the consumption rate per unit

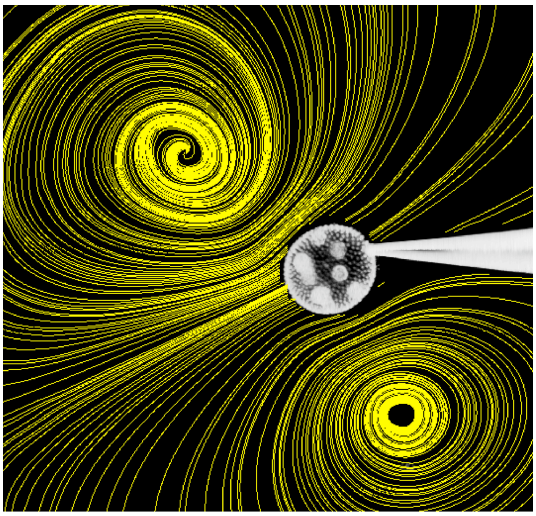

Figure 5: *Volvox* held on a micropipette, with streamlines visualized by particle-imaging-velocimetry. Diameter of colony is ~ 500 μm.

area. Clearly, there is a bottleneck radius $R_b = DC_\infty/\beta$ beyond which metabolic needs cannot be met by diffusion alone. Our estimates [23] suggest that this length scale is close to that at which the Volvocales display germ-soma differentiation (~ 150 μm). Since there are species much larger, there must be a means to increase nutrient acquisition accordingly. Indeed, we have recently established that the lineage covers a very broad range of Péclet numbers, from below unity at the single cell level, to vastly greater for colonies composed of thousands of cells. These large Péclet numbers arise from fluid flows driven by the coordinated action of tens, hundreds, or even thousands of flagella on the surface of these colonies, and imply metabolic dynamics fundamentally different from those limited by passive diffusion.

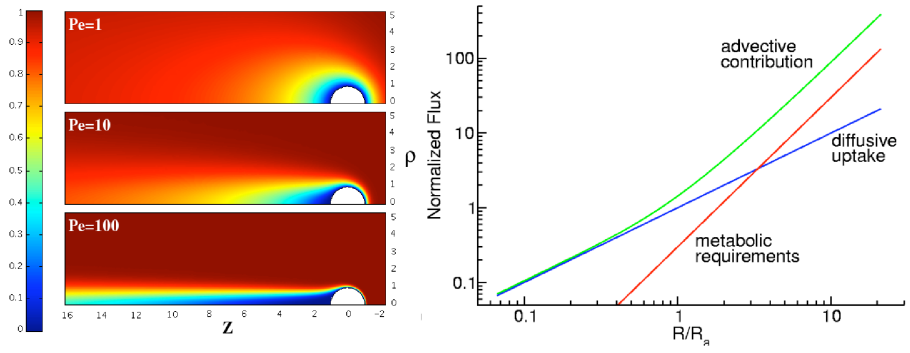

Figure 6: Results of finite-element computations of scalar concentration around an absorbing colony in flow at various Péclet numbers, showing boundary layer formation. (right) metabolite fluxes as a function of radius [23].

The concentration of a molecular species is governed by the equation

$$C_t + \mathbf{u} \cdot \nabla C = D\nabla^2 C \ , \tag{2}$$

for a solute concentration C in the presence of a fluid velocity field $\mathbf{u}$, with suitable boundary conditions. The key nontrivial point here is that $\mathbf{u}$ is a self-generated flow field

deriving from the complex flagellar dynamics. The exchange rates of such a scalar for large Péclet numbers were derived by Acrivos and Taylor [25] for the related problem of heat transfer from a solid sphere in a flow that is uniform far from the sphere, where it was found that the current scales as $\sim RPe^{1/3}$ for $Pe \gg 1$. The fractional exponent arises from a (thermal) boundary layer that hugs the sphere ever more tightly at higher velocities, thereby increasing the local thermal gradient and thus the heat flux. This particular scaling law is not directly applicable to the uptake problem of a solute because the boundary conditions for a flagellated alga are quite different from that of a solid sphere. Subsequent work by Magar, Goto, and Pedley [26, 27] and by us [23] showed that the alternative boundary conditions of either prescribed tangential velocity or prescribed tangential force distribution change the scaling law for the current of nutrients to $RPe^{1/2}$. The question then becomes: How does the self-generated fluid velocity scale with size? In a simple model for *Volvox* swimming [23], flagellar dynamics are summarized by a time-averaged tangential force per unit area f exerted on the fluid. This model predicts a characteristic flow velocity

$$U \sim \frac{\pi f R}{8\eta} \ , \tag{3}$$

where η is the fluid viscosity. Under this scaling, the Pe number grows with size as $UR \sim R^2$, and the uptake rate becomes $RPe^{1/2} \sim R^2$, bypassing the diffusional bottleneck (Fig. 6). This increase in nutrient uptake do to fluid flow driven by flagella serves not only to remove the diffusive bottleneck, but also to provide an evolutionary driving force for transitions to multicellularity. As seen in Fig. 6b, there is a nutrient uptake enhancement *per somatic cell* that arises from the collective flow. This increase is a very steep function of size for radii spanning from that of *Chlamydomonas* up to $100-200$ μm, the rough scale of germ-soma differentiation. One might say that this is socialism at work (!) - everyone stirs the fluid and everyone benefits.

4 Allometric Scaling of Flagella-Driven Flows

Because it is spherical, *Volvox* is an ideal organism for studies of biological fluid dynamics, being an approximate realization of Lighthill's "squirmer" model [28] of self-propelled bodies having a specified surface velocity. As mentioned above, such models have elucidated nutrient uptake at high Péclet numbers [26, 27, 23] by single organisms, and they have also illustrated pairwise hydrodynamic interactions between them [29]. Volvocine algae may also be used to study *collective* dynamics of self-propelled objects [30], complementary to bacterial suspensions (*E. coli, B. subtilis*) exhibiting large-scale coherence in thin films [31] and bulk [32].

We have investigated the scaling laws for flagella-driven flows in the Volvocales. Two allometric relations are key; (i) the fluid velocity (or swimming speed) of a colony as it grows and its somatic cells move further apart, and (ii) those velocities at a given somatic cell density as a function of colony diameter. Studies of a range of species over their life cycles yield data sets from which scaling laws can be tested.

The experimental methods are by now quite standard. *Volvox carteri* f. *nagariensis* EVE strain were grown axenically in Standard Volvox Medium [34] in diurnal growth chambers with sterile air bubbling, in a daily cycle of 16 h in cool white light ($\sim$ 4000 lux) at 28° C and 8 h in the dark at 26° C. Swimming was studied in a dual-view system (Fig. 7) [33], consisting of two identical assemblies, each a CCD camera (Pike 145B, Allied Vision Technologies, Germany) and a long-working distance microscope (InfiniVar CMS-2/S, Infinity Photo-Optical, Colorado). Dark-field illumination used 102 mm diameter circular LED arrays (LFR-100-R, CCS Inc., Kyoto) with narrow bandwidth emission at 655nm, to which *Volvox* is insensitive [35]. Thermal convection induced by the illumination

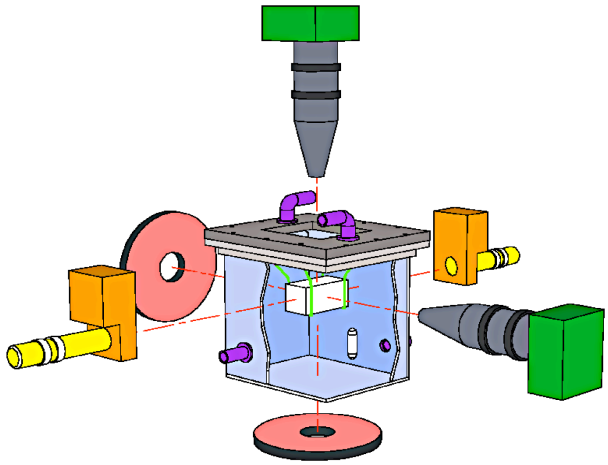

Figure 7: Schematic drawing of dual-view tracking apparatus [33]. The outer chamber (light blue, lid and flange in grey) contains a water bath, fed through inlets and outlets (purple), and mixed with a magnetic stir bar (white) driven by a motor external to the tank (not shown). The sample chamber (white) is suspended by stainless steel holders (light green), and illuminated by annular LED arrays (red). Microorganisms are visualized with two long-working-distance microscopes (dark gray) equipped with CCD cameras (dark green). Phototactic stimulus is provided by two LED and lens assemblies (yellow), and controlled by shutters (orange).

was minimized by placing the $2 \times 2 \times 2$ cm sample chamber, made from microscope slides held together with UV-curing glue (Norland), within a stirred, temperature-controlled water bath. Particle imaging velocimetry (PIV) studies (Dantec Dynamics, Skovelund, Denmark) showed that the r.m.s convective velocity within the sample chamber was $\lesssim 5$ μm/s.

From a theoretical point of view, four aspects of *Volvox* swimming are of interest, each arising, in the far field, from a distinct singularity of Stokes flow: (i) negative buoyancy (Stokeslet), (ii) self-propulsion (stresslet), (iii) bottom-heaviness (rotlet), and spinning (rotlet doublet). During the 48 hour life cycle, the number of somatic cells is constant; only their spacing increases as new ECM is added to increase the colony radius. This slowly changes the speeds of sinking, swimming, self-righting, and spinning, allowing exploration of a range of behaviors. The upswimming velocity U was measured with side views in the dual-view apparatus. *Volvox* density was determined by arresting self-propulsion through transient deflagellation with a pH shock [36], and measuring sedimentation. The settling velocity $V = 2\Delta\rho g R^2/9\eta$, with g the acceleration of gravity and η the fluid viscosity, yields the density offset $\Delta\rho = \rho_c - \rho$ between the colony and water. Bottom-heaviness implies a distance ℓ between the centers of gravity and geometry, measured by allowing *Volvox* to roll off a guide in the chamber and monitoring the axis inclination angle θ with the vertical, which obeys $\zeta_r \dot{\theta} = -(4\pi R^3 \rho_c g \ell/3) \sin\theta$, where $\zeta_r = 8\pi\eta R^3$ is the rotational drag coefficient, yielding a relaxation time $\tau = 6\eta/\rho_c g \ell$ [37]. The rotational frequencies ω_o of free-swimming colonies were obtained from movies taken from above, using germ cells/daughter colonies as markers.

Figure 8 shows the four measured quantities (U, V, ω_o, τ) and the deduced density offset $\Delta\rho$. In the simplest model [23], locomotion derives from a uniform force per unit area $\mathbf{f} = (f_\theta, f_\phi)$ exerted by flagella tangential to the colony surface. Balancing the net force $\int dS\, \mathbf{f} \cdot \hat{\mathbf{z}} = \pi^2 f_\theta R^2$ against the Stokes drag and negative buoyancy yields $f_\theta = 6\eta(U+V)/\pi R$. Balancing the flagellar torque $\int dS\, R\hat{\mathbf{r}} \times \mathbf{f} \cdot \hat{\mathbf{z}} = \pi^2 f_\phi R^3$ against viscous

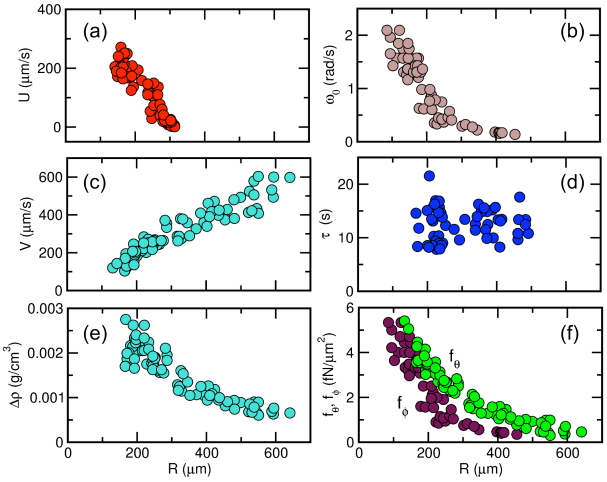

Figure 8: Swimming properties of *V. carteri* as a function of radius. (a) upswimming speed, (b) rotational frequency, (c) sedimentation speed, (d) reorientation time, (e) density offset, and (f) components of average flagellar force density.

rotational torque $8\pi\eta R^3\omega_o$ yields $f_\phi = 8\eta\omega_o/\pi$. These components are shown in Fig. 8f, where we used a linear parameterization of the upswimming data (Fig. 8a) to obtain an estimate of U over the entire radius range. The force density f_θ corresponds to several pN per flagellar pair [23], while the smallness of f_ϕ is a consequence of the $\sim 15^\circ$ tilt of the beating plane with respect to the colonial axis [38, 39].

These data provide a wealth of information on the physics of multicellular flagellar beating, and also provide the foundation for understanding some intriguing *collective* behavior of colonies. One such example is shown in Fig. 9. Here we see two colonies that have swum up to the ceiling of the experimental chamber and orbit about each other in a "hydrodynamic bound state" [40]. This configuration arises from the "infalling" of two colonies initially some distance apart at the ceiling. Their remarkable mutual attraction jarises from hydrodynamic interactions that are induced by the presence of the no-slip wall [41]. As each of the colonies spins about its axis it induces a short-range lubrication force on the other, slowing its motion and thereby producing a torque that leads to the orbiting motion. The fact that *Volvox* are bottom-heavy confers stability to this arrangement. A quantitative theory of the formation and dynamics of this bound state has been developed [40], making use of the extensive data in Fig. 8.

Hydrodynamic bound states, such as those described here, may have biological significance. When environmental conditions deteriorate, *Volvox* colonies enter a sexual phase of spore production to overwinter. Field studies show that bulk *Volvox* concentrations n are < 1 cm^{-3} [42], with male/female ratio of $\sim 1/10$, and ~ 100 sperm packets/male. Under these conditions, the mean encounter time for females and sperm packets is a substantial fraction of the life cycle. The hard sphere mean free path $\lambda = 1/\sqrt{2}n\pi(R+R_{sp})^2 \times 10/100$, with $R = 150$ μm for females, and $R_{sp} = 15$ μm for sperm packets, is $\lambda > 1$ m, implying a mean encounter time > 3 h. This suggests that another mechanism for fertilization must be at work, with previous studies having excluded chemoattraction in this system [43]. At naturally occurring concentrations, more than one *Volvox* may partake in the waltzing bound state, leading to long linear arrays (Fig. 9d). In such clusters, formed at the air-water interface, the recirculating flows would decrease the encounter times to seconds or minutes, clearly increasing the chance of sperm packets finding their intended target.

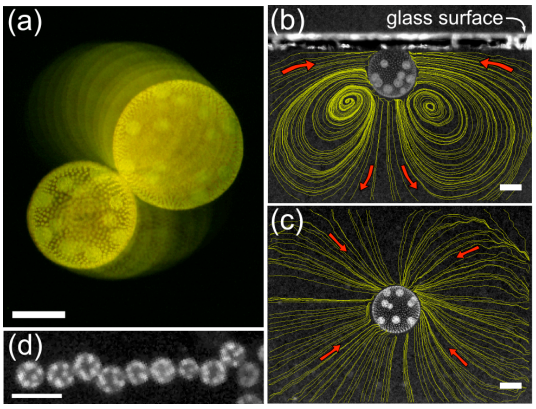

Figure 9: Waltzing of *V. carteri*. (a) Top view. Superimposed images taken 4 s apart, graded in intensity. (b) Side, and (c) top views of a colony swimming against a coverslip, with fluid streamlines. Scales are 200 μm. (d) A linear *Volvox* cluster viewed from above (scale is 1 mm).

5 Phototactic Steering

Another benchmark feature of the multicellularity exhibited by the Volvocales is their ability to perform accurate phototaxis, despite lacking a central nervous system to control the flagella beat dynamics. The accepted view of phototaxis [13] is that the light intensity measured by the photoreceptor of each individual somatic cell controls the beat dynamics its flagella (with strong beating at low light levels, weaker beating at high intensity). Much as plants grow toward light by elongating more on the dark side, this stronger beating on the dark side leads to phototaxis, although these responses to darkness and light are themselves transient. Of course, the persistent rotation of *Volvox* constantly brings new cells in and out of the dark and light sides, yielding a continuous modulation of the light response.

Since there have been no systematic simultaneous studies of phototactic trajectories and beat dynamics to quantify this process, we have begun to investigate these motions in detail. The dual-view tracking system is particularly useful in this regard, and has allowed us to obtain the preliminary data in Fig. 10. With this synchronization and the known relationship between light intensity, orientation, and flagellar beat patterns, the central mathematical questions which we aim to answer are both direct and inverse; Do the rules which are believed to connect light intensity to beat patterns lead to phototaxis as observed? What is the class of local rules relating light intensity to beat dynamics which produce phototaxis? Is there an optimum strategy?

6 Flagellar Synchronization

As noted long ago [44], coordinated beating of *Volvox* flagella is found in species with and those without cytoplasmic connections between somatic cells. This fact implicates hydrodynamic interactions in synchronization. Such interactions also appear to underlie the generation of metachronal waves on ciliates; in neither system has synchronization been adequately explained theoretically or quantified experimentally, although there is a growing body of work exploring the hydrodynamic origins [45, 46]. *Volvox* provides an excellent system to study this phenomenon, because of its ease of manipulation and visualization and the ability to sweep through a range of flagella lengths using the deflagellation technique mentioned earlier.

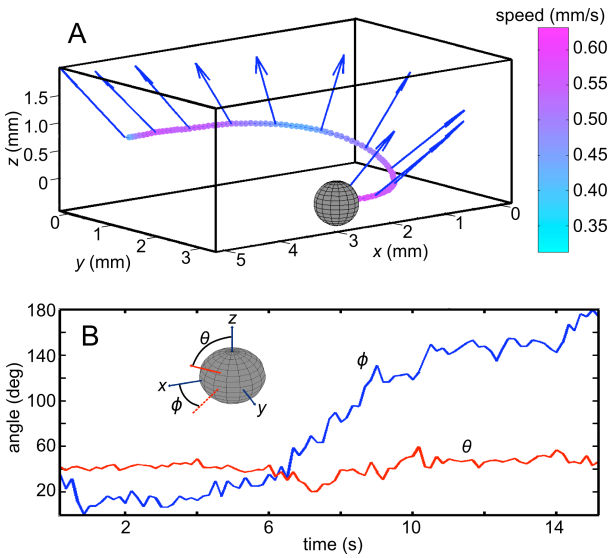

Figure 10: A phototactic turn of *Volvox barberi*. (a) The positional and orientational measurements are illustrated by vectors indicating the body axis, and swimming-speed-dependent coloration of the track. To initiate the 180° change swimming direction, the light initially was from the right along the x-axis and then changed to come from the left. Gravity is directed along the negative z-direction. Sphere represents initial position along the track. (b) Evolution of the body axis during the phototactic turn is described in terms of two angles θ and ϕ.

The ability to obtain high-resolution information on flagellar beating is illustrated in Fig. 11, where we see the two flagella on a single somatic cell of *Volvox* held on a micropipette. Imaging at up to 2000 video frames/sec allows a clear analysis of the waveform and precise measurement of the phase relationship between the two flagella.

One of the glaring lacunae in the theory of flagellar dynamics is a deep understanding of the synchronization of molecular motors via hydrodynamic interactions. A theory of synchronization has to be built from two main components: the hydrodynamic interactions between the moving objects (flagella) and the biochemical networks controlling the molecular motors which drive them. A point of reference for all such modeling is G.I. Taylor's well-known work on the hydrodynamic interactions between waving sheets in a viscous fluid [47], in which was solved the low Reynolds number fluid flow between two sheets undulating with specified traveling waves. It was found that the rate of viscous dissipation of energy was minimized when the two sheets undulated in phase. However, minimization of dissipation is not a dynamical principle with which to determine the state of a system. In the absence of a microscopic description of how the internal mechanism which produces the traveling wave responds to forces and torques from the adjacent sheet this question can not be answered.

The experimental situation is, however, becoming clearer. In recent work we have succeeded in tracking the flagellar beating dynamics of individual *Chlamydomonas* cells over thousands of beats, again with the help of the micromanipulation and imaging methods developed for *Volvox*. Historically [48], high-speed imaging of flagellar beating over periods of $1-2$ s have shown that the two flagella of intact cells beat in synchrony most of the time. Occasionally it has been found that there is an extra beat of one of the flagella, and very rarely one finds unsynchronized flagella displaying beat frequency differences of $10-30\%$. These different behaviors have been assumed to reflect variations between individual cells.

We have now shown that an individual *Chlamydomonas* cell can exhibit stochastic

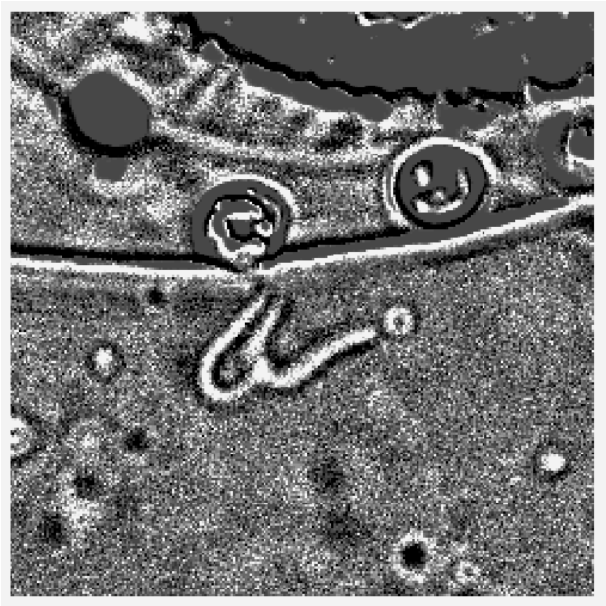

Figure 11: *Volvox* somatic cell flagella, imaged at 2000 frames per second. Image has been background-subtracted to enhance contrast.

transitions back and forth between the states of synchrony and asynchrony. In the synchronous state, the two flagella beat in phase for a period of time which is exponentially distributed with a mean of several seconds, interrupted by "phase slips" of either sign. One such phase slip (or extra beat) is shown in Fig. 12. The statistics of these phase slips are consistent with a very simple model of coupled phase oscillators in the presence of noise, allowing one to extract from the dynamics a good estimate of the intrinsic frequency difference between the two flagella in the phase-locked state. That difference is found to be a few percent. In the asynchronous state there is a clear phase difference of the magnitude known previously. This suggests strongly that the frequency difference between the flagella is dynamically regulated by the cell.

In addition, very recent experiments have shown that a consequence of this alternation between synchronous and asynchronous beating is the generation of a random walk in the trajectory of the cell. This, in turn, leads to diffusive behavior in a population of cells. In this sense, these findings show that there is a eukaryotic equivalent of the run-and-tumble locomotion well-known for peritrichously flagellated bacteria (e.g. *E. coli*) which swim by the rotation of helical flagella. The full implications of this finding for the life of these protists remains to be determined.

7 Conclusions

This overview has highlighted a number of challenging problems at the intersection biology, physics, and mathematics that are motivated by the dynamics of multicellularity. From understanding phototaxis of a multicellular flagellated protist to the synchronized beating of flagella coupled through hydrodynamics, much needs to be understood before we will have a clear picture of the evolutionary transition from unicellular to multicellular organisms.

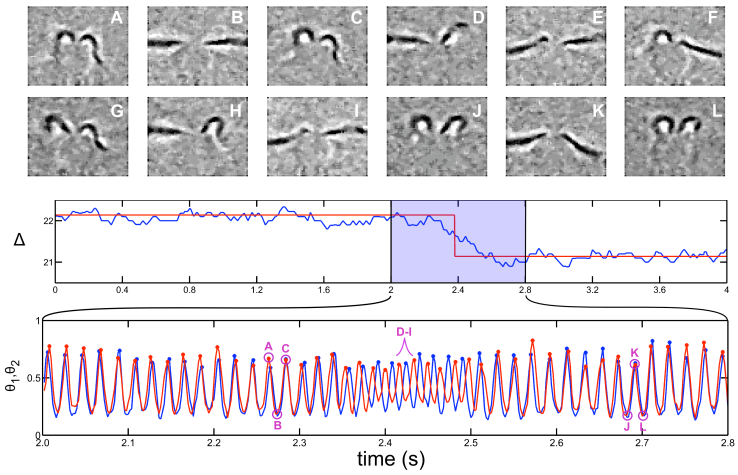

Figure 12: Phase slip in the beating of the two flagella of *Chlamydomonas*. (A-L) Individual movie frames. (b) Oscillatory signals obtained by local sampling of the image intensity near the flagella. (c) Phase difference between the two flagellar beats.

Acknowledgments

This overview highlights work done in collaboration with an extended group of physicists, applied mathematicians, and biologists: C.A. Solari, J.O. Kessler, R.E. Michod, M.B. Short, S. Ganguly, K. Drescher, I. Tuval, M. Polin, K. Leptos, T.J. Pedley, and T. Ishikawa. I am very grateful for support from the National Science Foundation, the Department of Energy, the Biotechnology and Biological Sciences Research Council, the Engineering and Physical Sciences Research Council, and the Schlumberger Chair Fund.

References

[1] J. Maynard Smith and E. Száthmary, *The Major Transitions in Evolution*, Freeman: San Francisco, 1995.

[2] J.T. Bonner, J. Biosci. **28** (2003), 523–528.

[3] J.T. Bonner, Evolution **58** (2004), 1883–1890.

[4] K.J.Niklas, *Plant Allometry*, University of Chicago Press: Chicago, IL, 1994.

[5] N. King, Develop. Cell **7** (2004), 313–325.

[6] G. Bell and A.O. Mooers, Biol. J. Linn. Soc. **60** (1997), 345.

[7] K.J. Niklas, Annals of Botany **85** (2000), 411–438.

[8] E. Guyon, J.P. Hulin, L. Petit, and C.D. Mitescu, Physical Hydrodynamics, Oxford University Press: Oxford, 2001.

[9] H.C. Berg and E.M. Purcell, Biophys. J. **20** (1977), 193–219.

[10] A. van Leeuwenhoek, Phil. Trans. Roy. Soc. **22** (1700), 509.

[11] C. Linneaus, *Systema Naturae*, 10th ed. (Holmiae, Impensis Laurentii Salvii, 1758), p. 820.

[12] A. Weismann, *Essays on Heredity and Kindred Biological Problems*, Oxford, Clarendon Press, 1892.

[13] D.L. Kirk, *Volvox: Molecular-genetic origins of multicellularity and cellular differentiation*, Cambridge University Press: Cambridge, 1998.

[14] A.W. Coleman, Proc. Natl. Acad. Sci. (USA) **96** (1999), 13892–13897.

[15] H. Nozaki, N. Ohta, H. Takano, and M.M. Watanabe, J. Phycology **35** (1999), 104–112.

[16] H. Nozaki, Biologa **58** (2003), 425–431.

[17] H. Nozaki, F.D. Ott, and A.W. Coleman, J. Phycol. **42** (2006), 1072–1080.

[18] A.G. Desnitski, Eur. J. Protist., **31** (1995), 241–247.

[19] D.L. Kirk, Ann. Rev. Gen. **31** (1997), 359–380.

[20] L.W. Tam and D.L. Kirk, Development **112** (1991), 571–580.

[21] A. Larson, M.M. Kirk, D.L. Kirk, Mol. Biol. Evol. **9** (1992), 85–105.

[22] C.A. Solari, S. Ganguly, J.O. Kessler, R.E. Michod, and R.E. Goldstein, Proc. Natl. Acad. Sci. (USA) **103** (2006), 1353–1358.

[23] M.B. Short, C.A. Solari, S. Ganguly, T.R. Powers, J.O. Kessler, and R. E. Goldstein, Proc. Natl. Acad. Sci. (USA) **103** (2006), 8315–8319.

[24] C.A. Solari, J.O. Kessler, and R.E. Michod, Am. Nat. **167** (2006), 537–554.

[25] A. Acrivos and T.D. Taylor, Phys. Fluids **5** (1962), 387–394.

[26] V. Magar, T. Goto and T.J. Pedley, Q. J. Mech. Appl. Math. **56** (2003), 65–91.

[27] V. Magar and T.J. Pedley, J. Fluid Mech. **539** (2005), 93–112.

[28] M.J. Lighthill, Commun. Pure Appl. Math. **5** (1952), 109.

[29] T. Ishikawa and M. Hota, J. Exp. Biol. **209** (2006), 4452; T. Ishikawa, M.P. Simmonds, and T.J. Pedley, J. Fluid Mech. **568** (2006), 119.

[30] T. Ishikawa and T.J. Pedley, Phys. Rev. Lett. **100** (2008), 088103; T. Ishikawa, J.T. Locsei, and T.J. Pedley, J. Fluid Mech. **615** (2008), 401.

[31] X.-L. Wu and A. Libchaber, Phys. Rev. Lett. **84** (2000), 3017 ; A. Sokolov, *et al.*, Phys. Rev. Lett. **98** (2007), 158102.

[32] C. Dombrowski, *et al.*, Phys. Rev. Lett. **93** (2004), 098103.

[33] K. Drescher, K. Leptos, and R.E. Goldstein, Rev. Sci. Instrum. **80** (2009), 014301.

[34] D.L. Kirk and M.M. Kirk, Dev. Biol. **96** (1983), 493.

[35] H. Sakaguchi and K. Iwasa, Plant Cell Physiol. **20** (1979), 909.

[36] G.B. Witman, *et al.*, J. Cell Biol. **54** (1972), 507.

[37] T.J. Pedley and J.O. Kessler, Ann. Rev. Fluid Mech. **24** (1992), 313.

[38] H.J. Hoops, Protoplasma **199** (1997), 99.

[39] K. Drescher, et al., preprint (2009).

[40] K. Drescher, et al., submitted (2009).

[41] J.R. Blake, Proc. Camb. Phil. Soc. **70** (1971), 303–310.

[42] F. DeNoyelles, Jr., Ph.D. thesis, Cornell Univ. (1971).

[43] S.J. Cogging, *et al.*, J. Phycol. **15** (1979), 247.

[44] J.D.F. Hiatt and W.G. Hand, J. Protozool. **19** (1972), 488–489.

[45] A. Vilfan and F. Jülicher, Phys. Rev. Lett. **96** (2006), 058102.

[46] B. Guirao and J.-F. Joanny, Biophys. J. **92** (2007), 1900–1917.

[47] G.I. Taylor, Proc. Roy. Soc. A **209** (1951), 447–461.

[48] U. Rüffer and W. Nultsch, Cell. Mot. **7** (1987), 87; **15** (1990), 162; **18** (1991), 269; **41** (1998), 297.

[49] M. Polin, *et al.*, preprint (2009).